Dependence of *trans*-1-(2-Anthryl)-2-phenylethene Conformer-Specific Fluorescence Spectra and Fumaronitrile Quenching Rate Constants on Temperature

Jack Saltiel,* Yuxin Zhang, and Donald F. Sears, Jr.

Department of Chemistry, The Florida State University, Tallahassee, Florida 32306-3006

Received: November 8, 1996; In Final Form: July 4, 1997[⊗]

The quenching of *trans*-1-(2-anthryl)-2-phenylethene (*t*-APE) fluorescence by fumaronitrile (FN) was determined as a function of excitation wavelength (λ_{exc}) and temperature ($5.0 \leq T \leq 80.0$ °C). Principal component analysis with self-modeling (PCA-SM) was applied separately to the fluorescence spectra at each temperature. Resolved pure conformer fluorescence spectra were based on the condition that Stern−Volmer quenching constants for each conformer be λ_{exc}-independent. A shoulder at the blue edge of the spectra of the more extended, s-trans conformer (*t*-APE_B) becomes more pronounced with increasing temperature revealing fluorescence from a thermally populated S_2 state. Similar, but more subtle changes are evident in the spectra of the s-cis conformer (*t*-APE_A). Both sets of resolved spectra exhibit blue shifts and broadening as the temperature is increased. These spectral changes are reflected in the shape of the eigenvectors obtained from the PCA of each set of spectra and prevent their resolution into $S_2 \rightarrow S_0$ and $S_1 \rightarrow S_0$ components. An earlier PCA-SM based resolution of a *t*-APE spectrothermal matrix into $S_1 \rightarrow S_0$ fluorescence of *t*-APE_A and $S_2 \rightarrow S_0$, $S_1 \rightarrow S_0$ fluorescence spectra of *t*-APE_B is evaluated.

Introduction

The adherence of the photophysical behavior of *trans*-1-(2-anthryl)-2-phenylethene (*t*-APE) to Havinga's NEER (non-equilibration of excited rotamers) principle[1] is well established.[2−5] We have described the resolution of the fluorescence, fluorescence-excitation, and absorption spectra in toluene solution of *t*-APE_A and *t*-APE_B, the two *t*-APE conformers,[4] and presented a

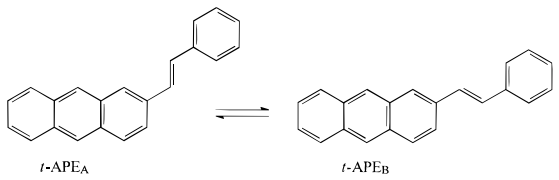

critical comparison of our results with those of earlier workers.[2,3] However, the results of our spectral resolution and our conclusions have been questioned recently.[5]

Conformer-specific adiabatic ^1c-$APE_B^* \rightarrow {}^1t$-$APE_B^*$ isomerization was first proposed by Mazzucato et al. based on preliminary fluorescence observations on *c*-APE in methylcyclohexane/3-methylpentane (MCH-3MP) solutions.[6] Our independent study of *c*-APE fluorescence in toluene established that this adiabatic pathway accounts for at least 44% of initially excited ^1c-APE_B* at 20 °C.[7] No evidence could be found for the corresponding process in ^1c-APE_A*,[6] which based on a report on a methyl derivative[8] undergoes conformer-specific cyclization to the corresponding dihydrophenanthrene. This behavior is entirely analogous to that of the 2-naphthyl analogue, *cis*-1-(2-naphthyl)-2-phenylethene (*c*-NPE), except that the adiabatic isomerization of the B conformer is more than 20 times more efficient in APE.[9] The highly efficient conformer-specific adiabatic $^1c^* \rightarrow {}^1t^*$ isomerization of *c*-APE_B may reflect a short residence time of the excited molecule at the perpendicular geometry, ^1p_B*. Semiempirical quantum mechanical calculations predict that $^1p_A^*$ in the APE_A conformer is the transition state along the $^1c^* \rightarrow {}^1t^*$ reaction coordinate and that its energy relative to $^1c^*$ is sufficiently high, 12−16 kcal/mol, as to preclude adiabatic $^1c^* \rightarrow {}^1t^*$ isomerization.[3a] Calculations on the energetics of torsional motion along the ethylenic bond of $^1APE_B$* have not been reported. However, based on the rate constant for radiationless decay of ^1c-APE_B* in toluene at 20 °C, the activation energy barrier along the $^1c_B^* \rightarrow {}^1t_B^*$ coordinate has been estimated as ≤7 kcal/mol.[7] The temperature dependencies of the fluorescence quantum yield and lifetime of ^1c_B* and of the efficiency of the $^1c_B^* \rightarrow {}^1t_B^*$ process should provide a more accurate empirical measure of the magnitude of this barrier, and may also reveal whether ^1p_B* corresponds to an intermediate or to a transition state along the torsional coordinate.

Resolution of fluorescence spectra of *c*-APE toluene solutions at 20 °C[6] was based on the known fluorescence spectrum of *t*-APE_B and the known Stern−Volmer constant, K_{SV}^B, for O_2 quenching of the fluorescence of *t*-APE_B.[4] Extension of this work to other temperatures requires knowledge of the spectra and K_{SV} values of the *t*-APE conformers at each temperature. Fluorescence spectra of *t*-APE_B in toluene are known to be strongly temperature dependent.[3b−d] Especially noticeable is a shoulder at 395 nm that is absent at 147 K but gains in intensity as the temperature is raised to 360 K.[3b−d] This shoulder has been attributed to $S_2 \rightarrow S_0$ emission of the *t*-APE_B conformer which arises due to thermal population of the nearby S_2 ($\Delta E_{S_2-S_1} = 1.80$ kcal/mol[3c]) state and has a higher oscillator strength than does S_1. The presence of nearly degenerate S_1 and S_2 states with widely different oscillator strengths had been predicted theoretically for both *t*-APE conformers.[3a] A PCA-SM based resolution of a *t*-APE spectrothermal matrix into $S_1 \rightarrow S_0$ fluorescence of *t*-APE_A and $S_2 \rightarrow S_0$ and $S_1 \rightarrow S_0$ dual fluorescence from *t*-APE_B has been published.[3d] However, its validity has been questioned because possible blue shifts and broadening of the individual conformer spectra were disregarded.[4] Nonlinear spectral changes can control the outcome of PCA-SM calculations leading to invalid spectral assignments

[⊗] Abstract published in *Advance ACS Abstracts,* August 15, 1997.

S1089-5639(96)03734-6 CCC: $14.00

especially when temperature changes cause only minor perturbations in conformer composition due to small free energy differences between the equilibrating species.[10]

The present work is motivated by the desire to obtain pure *t*-APE conformer spectra at different temperatures as a prelude to the study of the temperature dependence of conformer specific adiabatic ^1c-APE$_B$* $\rightarrow$ ^1t-APE$_B$* isomerization. Fumaronitrile, FN, a strong electron acceptor, was substituted for O_2 in applying the SV constant criterion in these resolutions because its concentration is easier to control at different temperatures and because the results may be valuable in a future study of site and conformer selectivity in its photoreactions with *t*-APE. The independent determination of the fluorescence spectrum of *t*-APE$_A$ should resolve the controversial aspects of this assignment.[3-5] Finally, determination of the temperature effects on the *t*-APE$_A$ and *t*-APE$_B$ fluorescence spectra, separately, should allow a more meaningful evaluation of the earlier attempt to resolve *t*-APE$_B$ fluorescence into $S_2 \rightarrow S_0$ and $S_1 \rightarrow S_0$ components.[3d]

Experimental Section

Materials. Toluene and *t*-APE were as previously described.[7] Fumaronitrile (Aldrich) was recrystallized from benzene prior to use.

Absorption Spectra. Absorption spectra were measured using a Perkin-Elmer Lambda-5 spectrophotometer interfaced with a Dell Corp. 12-MHz 80286/87 microcomputer.

Fluorescence Spectra. Fluorescence spectra were measured using an extensively modified Hitachi/Perkin-Elmer MPF-2A spectrophotometer as previously described.[10] Quartz cells, constructed from square 1-cm precision-bore tubing (Ace Glass), were attached via ground seals to Pyrex degassing bulbs (13 mm o.d. tubing) fitted with 10/30 standard-taper joints and grease traps. Solutions, 4.0 mL, were degassed by use of five freeze−pump−thaw cycles to about 10^{-5} Torr, after which the ampules were flame-sealed at a constriction. Solutions were transferred to the square cells, and emission spectra were recorded following temperature equilibration in the thermostated cell compartment. Following each set of measurements, the cells were broken open, cleaned, and the measurements repeated with pure solvent.

Data Analysis. Principal component analysis with self-modeling calculations were performed on a PC-s limited Dell 80486/87 (25 MHz) microcomputer as previously described.[4,10]

Results

Spectral Sets. Three separate sets of *t*-APE/FN solutions in toluene were employed in order to minimize changes in concentration due to possible photoreaction in the course of the fluorescence measurements. In the initial experiment, intended to test our previously published spectral resolution of *t*-APE$_A$ and *t*-APE$_B$ fluorescence spectra, fluorescence spectra were measured at 19.3 °C for [*t*-APE] = 1.91×10^{-6} M and [FN] = 0.0, 1.01×10^{-3}, 4.16×10^{-3}, and 8.25×10^{-3} M. Emission spectra were recorded in the 360−580 nm range in 0.5 nm increments for λ_{exc} = 352, 362, 372, 382, 392, and 402 nm. In the second and third experiments, collection of distilled solvent in the degassing bulbs at $T \geq 59.3$ °C was avoided by connecting the bulbs to the fluorescence cell at an angle greater than 90°. In the second experiment, measurements were carried out at 4.3, 39.3, 59.3, and 79.3 °C for [*t*-APE] = 1.91×10^{-6} M and [FN] = 0.0, 1.14×10^{-3}, 2.18×10^{-3}, and 3.32×10^{-3} M (concentrations at 19.3 °C). In the third experiment, concentrations at 19.3 °C were [*t*-APE] = 1.02×10^{-6} M and [FN] = 0.0, 0.989×10^{-3}, 1.98×10^{-3}, 2.97×10^{-3}, and 3.96×10^{-3} M. An additional excitation wavelength, 406 nm, was employed and measurements were carried out at 19.3, 59.3, 69.3, and 79.3 °C. In all cases, absorption spectra measured before and after the fluorescence measurements showed no discernible changes in solute concentrations. The net absorbance of FN, integrated over the 300.0−310.0 nm range, was employed to correct concentrations for loss of solvent during the degassing procedure. This absorbance is absent when FN is dissolved in methylcyclohexane. Consequently, it is probably due to a ground state FN/toluene complex. Upward adjustments of [FN] ranged from 1.1 to 8.6% with the average for 10 solutions being 4.8%. In applying the Stern−Volmer constant constraint, FN concentrations were adjusted for solvent density variation with temperature.

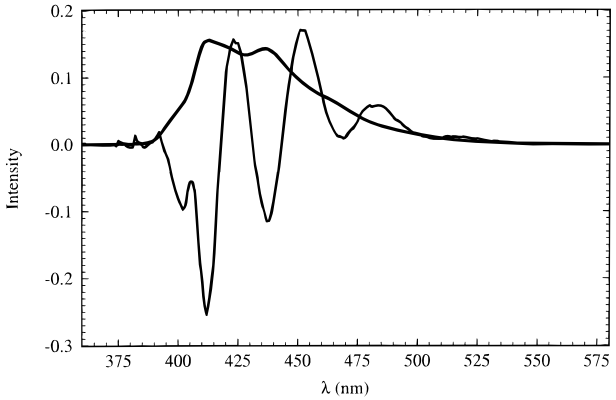

Figure 1. Eigenvectors of *t*-APE/FN fluorescence matrix at 19.3 °C. The four largest eigenvalues are 4.047×10^{-1}, 1.376×10^{-3}, 6.433×10^{-6}, and 3.888×10^{-6}. The two eigenvectors shown account for 99.99% of the total variance.

Spectral Resolutions. Background correction of the fluorescence spectra was achieved as previously described.[7] Corrections for self-absorption were unnecessary at the low *t*-APE concentrations employed. PCA was applied separately to the spectra at each temperature. Minimization of the standard deviation from the global Stern−Volmer plot of each conformer was relied upon as the SM criterion.[4,11] Since our earlier resolution at 20 °C (subsequent recalibration of the temperature detector showed this temperature to be 19.3 °C), based on O_2 as the fluorescence quencher, has been questioned, we describe here the first resolution (experiment 1) at 19.3 °C in detail. This resolution was repeated in an independent experiment at the conclusion of this study (experiment 3). The input matrix (24 × 221) consisted of 24 spectra (6 λ_{exc} at each of 4 [FN]) with intensities entered at each 1.0 nm interval in the 360−580 nm range. As in earlier PCA-SM applications, the matrix consisted of fluorescence spectra uncorrected for nonlinearity in instrumental response. This correction was applied to the derived pure component spectra as the final step in the procedure. The resulting significant eigenvectors and corresponding eigenvalues are shown in Figure 1. Combination coefficients of the experimental spectra adhere closely to the normalization line on which pure component coefficients are also shown based on well-defined minima on the standard deviation plots for the global Stern−Volmer plots (Figure 2). The corresponding Stern−Volmer plots and pure component spectra are shown in Figures 3 and 4, respectively. Repetition of this procedure for each temperature yielded the temperature dependence of pure component Stern−Volmer plots and pure component *t*-APE$_A$ and *t*-APE$_B$ spectra (Figures 5 and 6). The Stern−Volmer constants are summarized in Table 1. Also shown in Table 1 is the variation of the density and viscosity of toluene with temperature.[12]

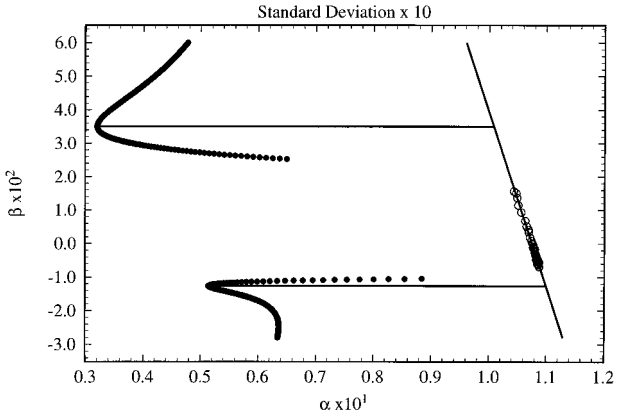

Figure 2. Normalization line and combination coefficients for the 19.3 °C spectral matrix. The curves give standard deviation/slope ratios for the global Stern−Volmer plots.

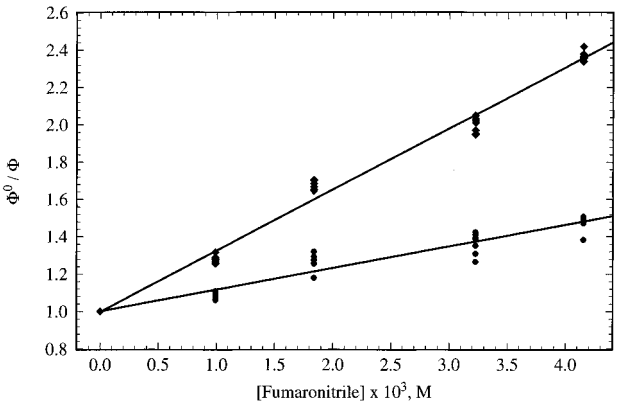

Figure 3. Global Stern−Volmer plots for FN quenching of resolved *t*-APE$_A$ (●) and *t*-APE$_B$ (◆) fluorescence in toluene at 19.3 °C.

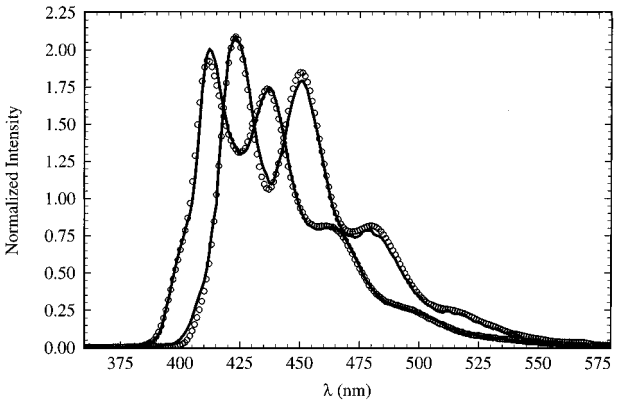

Figure 4. Pure component *t*-APE$_A$ (longer λ) and *t*-APE$_B$ (shorter λ) fluorescence spectra in toluene at 19.3 °C based on the optimum SV limits in Figure 3. The points show the resolved spectra at 19.3 °C from ref 4. All spectra are corrected for nonlinearity in instrumental response.

Discussion

A brief review of earlier work[2,3] on the manifestations of rotamerism on the fluorescence spectra and decay rate constants of *t*-APE was presented in our recent paper.[4] Relatively good agreement between our resolved conformer spectra[4] and those obtained earlier by Spalletti et al.[3d] was observed for the fluorescence spectrum of *t*-APE$_A$ and for the fluorescence-excitation spectrum of *t*-APE$_B$. However, the fluorescence spectra for *t*-APE$_B$ and the fluorescence-excitation spectra of *t*-APE$_A$ from the two studies showed unacceptable discrepancies.[4] The first PCA-SM resolution was based on the Lawton and Sylvestre (LS) nonnegativity constraint,[3d] whereas ours included the Stern−Volmer (SV) constant optimization constraint.[4] In the SV method the quencher concentration effect on the spectra serves as an additional experimental dimension that, provided the SV constants of the two conformers are not fortuitously identical, is capable of defining the combination coefficients of the pure component spectra uniquely.[4,11,13] The LS procedure succeeds in defining the pure component spectra uniquely only when spectral regions exist where only a single component contributes. This condition cannot be known to be satisfied a priori, and even when it is satisfied, the exact extent of spectral nonoverlap is unknown. It follows that for a two-component system the LS method generally defines two ranges of potential pure component spectra that correspond to the combination coefficients of the two outer segments of the normalization line starting with those of the experimental spectra richest in a specific component and ending at the outer LS

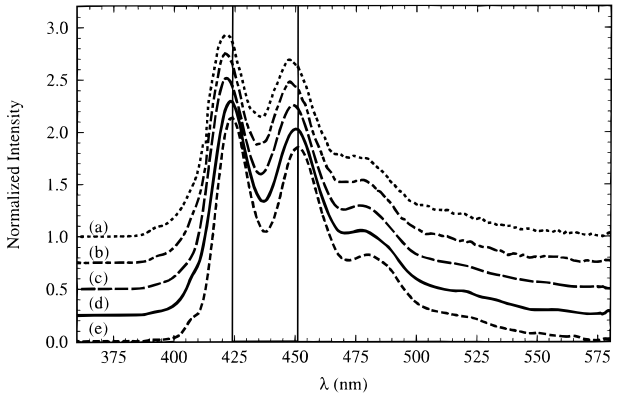

Figure 5. Pure component *t*-APE$_A$ fluorescence spectra at 79.3, 69.3, 59.3, 39.3, and 4.3 °C in the order (a) to (e). Spectra are corrected for nonlinearity in instrumental response.

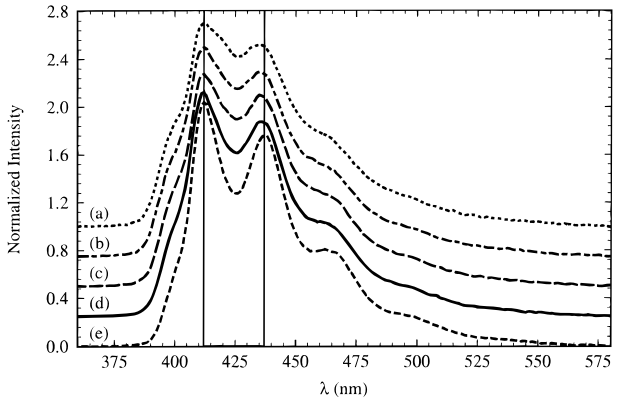

Figure 6. Pure component *t*-APE$_B$ fluorescence spectra as in Figure 5.

TABLE 1: Conformer-Specific Stern−Volmer Constants for the Quenching of *t*-APE Fluorescence by FN in Toluene[a]

T, °C	K_{SV}^A, M^{-1}	K_{SV}^B, M^{-1}	*d*, g/mL	$10^3\eta$, P
4.3	80.3 (3.1)	265.9 (5.5)	0.8881	7.22_5
19.3	116.4 (2.8)	347.8 (3.3)	0.8663	5.92_3
	115.5 (5.3)	328.7 (6.4)		
39.3	155.2 (5.7)	460.5 (8.4)	0.8476	4.69_3
59.3	214.7 (10.5)	567.0 (15.2)	0.8285	3.82_8
	220.0 (12.8)	528.0 (11.5)		
69.3	277.5 (14.1)	617.0 (12.5)	0.8188	3.48_7
79.3	310.8 (22.9)	648.3 (24.8)	0.8088	3.19_3
	248.1 (29.6)	604.9 (12.7)		

[a] Stern−Volmer constants are based on slope/intercept ratios of Stern−Volmer plots and are thus corrected for small deviations of intercepts from unity; values in parentheses are standard deviations in the last significant figures shown.

combination coefficients beyond which negative spectral contributions exceeding random experimental noise are encountered. In the case of *t*-APE, *t*-APE_B has long been known to contribute uniquely at the onset of the mixture fluorescence spectra.[2,3] Consequently, the LS procedure, within noise limitations, should exactly define the fluorescence spectrum of *t*-APE_A at the outer LS combination limit that corresponds to baseline signal at the onset of the spectral range. This accounts for the good agreement between the *t*-APE_A fluorescence spectra from the LS procedure[3,4] and that obtained by the SV procedure using O_2 as the fluorescence quencher.[4] Our results from the two methods were compared in Figure 4 of ref 4 where it was pointed out that due to the slightly negative intensities at the onset of the SV spectrum, the LS *t*-APE_B spectrum was considered more accurate.

The choice of FN as the quencher in this study was based, in part, on earlier reports that it is a highly efficient quencher of the fluorescence of *trans*-stilbene[14] (*t*-S) and of related 1,2-diarylethenes.[15] The exciplex fluorescence observed for the *t*-S/FN system in nonpolar solvents ($\tau = 13$ ns in benzene)[14] is identical to that obtained upon direct excitation of the ground state charge transfer complex that forms ($K = 0.5\ M^{-1}$) at high *t*-S/FN concentrations.[16] In nonpolar solvents this species is a contact radical ion pair[14−16] as has been established by transient absorption measurements.[14c,17] At the relatively low [FN] employed in our work no manifestations of ground state complexation or exciplex formation are discerned. Absorption spectra of FN/*t*-APE mixtures are strictly additive with respect to the individual components and *t*-APE fluorescence spectra in the presence of our highest [FN] are reproduced faithfully using the eigenvectors from ref 4.

Comparison of the LS spectra for *t*-APE_A from ref 4 with the SV spectrum obtained in this work from two independent experiments using FN as the quencher at 19.3 °C again shows them to be in excellent agreement (Figure 4). The somewhat noisier appearance of the new spectra is a consequence of larger noise to signal ratios in the experimental spectra reflecting the lower *t*-APE concentrations employed in this work. Examination of Figure 4 shows that vibronic structure in the spectrum of *t*-APE_B is less well resolved than in the spectrum of *t*-APE_A. This is in part due to the overlap of the $S_2 \rightarrow S_0$ emission on the dominant $S_1 \rightarrow S_0$ emission of this conformer (as evident in the shoulder at the onset of the spectrum)[3], and in part on the broader nature of the $S_1 \rightarrow S_0$ emission. As a result, the spectral region at the tail portion of the spectra where *t*-APE_A contributes uniquely is not clearly defined. This leads to a large uncertainty in defining the LS outer limit combination coefficients for the fluorescence spectrum of *t*-APE_B. The SV procedure, on the other hand, defines the fluorescence spectrum of *t*-APE_B more narrowly on optimizing global SV plots for *t*-APE_A. Figure 4 shows that the independently obtained spectra of *t*-APE_B based on O_2 and on FN fluorescence quenching at 19.3 °C are in excellent agreement. The combination coefficients of these pure component spectra fall within the range of acceptable LS spectra in both cases but are far from the combination coefficients of the LS outer limit spectrum that was assigned to *t*-APE_B first by Spalletti et al.[3d] and more recently by Bartocci et al.[5] Having confirmed our initial spectral assignments,[4] we conclude, once again, that at least in toluene, the alternative assignments of Spalletti, Bartocci, and co-workers are not valid.[3d,5] The discrepancies are due to the arbitrary assumptions that were made by these workers concerning the widths of the regions of spectral nonoverlap between the fluorescence spectra of the two conformers at the onset and tail portions of the spectra. Incorrect identification of the pure component combination coefficients on the normalization line leads to incorrect fractional contributions of the components, x_A and x_B, to the experimental spectra, and, in turn, to incorrect pure component fluorescence excitation spectra.[4,11]

In their investigation of the discrepancies between the spectral resolutions in refs 3d and 4,[5] Bartocci et al. also applied an independent resolution method based on quantitative kinetic fluorescence analysis (KFA).[18] Since the KFA approach yielded resolved spectra in nearly exact agreement with those based on their PCA-SM resolution, it is important to consider how these two seemingly independent approaches may lead to identical erroneous spectra. As applied in ref 5, the KFA procedure[18] requires identification of isoemissive wavelengths, λ'_{em}, at which the decay kinetics are monitored. Since at these wavelengths the two conformers contribute equally to the observed fluorescence intensity, independent of λ_{exc}, identification of λ'_{em} requires measurement of accurate composite fluorescence quantum yields, $\bar{\phi}_f$, as a function of λ_{exc}. Provided that the pure component fluorescence quantum yields, ϕ_{f_B} and ϕ_{f_B}, are independent of λ_{exc}, normally a safe assumption, the quantitative relationship between $\bar{\phi}_f$ and x_A is given by[4,11]

$$\frac{1}{\bar{\phi}_f(\lambda_{exc})} = \frac{1}{\phi_{f_B}} + \left(\frac{1}{\phi_{f_A}} - \frac{1}{\phi_{f_B}}\right) x_A(\lambda_{exc}) \qquad (1)$$

Our plot of the extensive set of $\bar{\phi}_f$ values for toluene at 20 °C from ref 3d based on eq 1 showed significant deviations from linearity, particularly for values in the 0.76−0.83 range corresponding to $340 \leq \lambda_{exc} \leq 372$ nm.[4] For these λ_{exc} range x_A is ≤0.2 and, as a result, a relatively low $\phi_{f_B} = 0.81$ was predicted (compare with $\phi_{f_A} = 1.00$).[3d,4] The new set of $\bar{\phi}_f$ values that was reported recently[5] agrees well with the previous set and similarly fails to adhere to eq 1. In fact, it led Bartocci et al. to adjust downward the quantum yield of *t*-APE_B to $\phi_{f_B} = 0.76$.[5] Measurement of accurate $\bar{\phi}_f$ values for *t*-APE is difficult especially when 9,10-diphenylanthracene (DPA) is employed as standard.[5] This is because the steep slopes in the absorption spectra of *t*-APE and of DPA cause large absorbance errors to be associated with small uncertainties in λ_{exc}. Our fluorescence quantum yield measurements with quinine bisulfate as the standard have yielded a significantly larger $\bar{\phi}_f = 0.89$ for $\lambda_{exc} = 340$ and 344 nm[7] for which $x_A \simeq 0.08$.[4] This value has led us to adjust ϕ_{f_B} to 0.88.[7] It is not surprising, therefore, that $\lambda_{em} = 443$ nm, selected in ref 5 as the isoemissive wavelength on which the KFA resolution was based, is not an isoemissive wavelength based on our results. Since different spectra were assigned to the two components in the two studies, and since these spectra are, in addition, scaled to different relative areas based on different ϕ_{f_A}/ϕ_{f_B} ratios, the crossing points (λ'_{em}) must of necessity be different.

Temperature Effects: Stern−Volmer Constants. The biexponential decay of *t*-APE_A in toluene has been analyzed in the 193−353 K temperature range.[3b] The fluorescence lifetimes of the two components are remarkably insensitive to temperature, reflecting nearly unity fluorescence quantum yields. The small decreases in τ_{f_A} and τ_{f_B} as the temperature is lowered are consistent with the expected dependence of the radiative rate constants, k_{f_A} and k_{f_B}, on the refractive index of the medium.[19] These decreases in τ_f are not strictly monotonic and may also reflect changes in the S_2—S_1 energy gaps in the two conformers (see below). The lifetimes[3b] together with our SV constants give the temperature dependence of the conformer specific FN quenching rate constants, k_{qA}^{FN} and k_{qB}^{FN}, (Table 2).

The rate constants at 19.3 °C are 1.41×10^{10} and $1.21 \times 10^{10}\ M^{-1}\ s^{-1}$ for FN quenching of ^{1}*t*-APE_A* and ^{1}*t*-APE_B*,

TABLE 2: Conformer-Specific Rate Constants for the Quenching of *t*-APE Fluorescence by FN in Toluene[a]

T, °C	$10^9\tau_{f_A}$, s^{-1}	$10^9\tau_{f_B}$, s^{-1}	$10^{-10}k_{q_A}^{FN}$, $M^{-1}\,s^{-1}$	$10^{-10}k_{q_A}^{FN}$, $M^{-1}\,s^{-1}$
4.3	7.7	26.3	1.04	1.01
19.3	8.2	28.0	1.41	1.21
39.3	8.2	27.8	1.89	1.66
59.3	8.2_5	27.8	2.65	1.97
69.3	8.3	27.8	3.34	2.22
79.3	8.3	27.8	3.37	2.25

[a] Fluorescence lifetimes are interpolated values from ref 3b; k_q values are based on average K_{SV} values from Table 1.

respectively. These values are well within a factor of 2 of expected diffusion-controlled rate constants.[20] Specifically, use of the benzyl radical coupling reaction in toluene as a standard reaction and ignoring small differences in encounter distances, σ, and mutual diffusion coefficients, D, gives $k_{diff}^0 = 1.87 \times 10^{10}$ M^{-1} s^{-1} as the expected rate constant at 20 °C in the absence of transient effects.[20,21] The transient terms in the Smoluchowski equation for a diffusion-controlled reaction cannot be neglected in reactions of excited species whose lifetimes are shorter than 10^{-6} s.[22,23] This probably accounts, at least in part, for the anomalously high rate constant, $\sim 7 \times 10^{10}$ M^{-1} s^{-1}, that can be inferred from the SV constant for FN quenching of the very short lived (~0.10 ns) ^1t-S* fluorescence.[14] The contribution of the transient term is highly dependent on the lifetime of the excited species. For instance, in the case of *N*,*N*-dimethylaniline quenching of anthracene fluorescence, $\tau_f^0 = 5.2$ ns, in cyclohexane it augments the rate constant derived from the standard SV plot by ~30%.[23] A derived relationship between the effective diffusion-controlled rate constant, k_{diff}, and the lifetime of the quenched excited state[24]

$$k_{diff} = k_{diff}^0\left(1 + \frac{\sigma}{D^{1/2}\tau_f^{01/2}}\right) \qquad (2)$$

was applied recently in estimating the lifetime of the T_2 state of anthracene from the SV constant of its quenching by a 1,3-diene.[25] The $(\sigma/\sqrt{D}) = 1.88 \times 10^{-5}$ $s^{1/2}$ value used in this calculation[25] was based on an unrealistically low assumed value for D (see Table 16 in ref 20). Nonetheless, with the use of this value eq 2 predicts $k_{diff} = 1.26k_{diff}^0$ for $\tau_f^0 = 5.2$ ns in good agreement with the experimentally observed ~30% enhancement. For our system, the calculated k_{diff} values are $1.21k_{diff}^0$ and $1.11k_{diff}^0$ for $\tau_f^0 = 8$ (^1t-APE$_A$*) and 28 ns (^1t-APE$_B$*), respectively. For the ^1t-St*/FN system the predicted enhancement for $\tau_f^0 = 0.10$ ns is substantial, $k_{diff} = 2.9k_{diff}^0$, and goes a long way toward accounting for the experimentally derived rate constant. It is likely, in view of the very high [FN] employed in the latter study,[14] that static quenching also contributes in the *t*-S case. It seems reasonable to conclude that the somewhat larger quenching constant obtained for ^1t-APE$_A$ relative to ^1t-APE$_B$ reflects the greater contribution of the transient term in the former. Of course, use of the more realistic $D \simeq 4 \times 10^{-7}$ dm^2 s^{-1} in eq 2[20] substantially diminishes (by a factor of ~2) the predicted contribution of the transient term.

In terms of Eyring's transition state theory the quenching rate constants $k_{q_i}^{FN}$, where *i* designates conformer A or B, are given by

$$k_{q_i}^{FN} = \left(\frac{\kappa_i kT}{\eta}\right)e^{\Delta S_i^{\ddagger}/R}e^{-\Delta H_i^{\ddagger}/RT} \qquad (3)$$

where the $\Delta H_i^{\ddagger}$ are the enthalpies of activation, the $\Delta S_i^{\ddagger}$ are the entropies of activation, and the κ_i's are transmission factors.

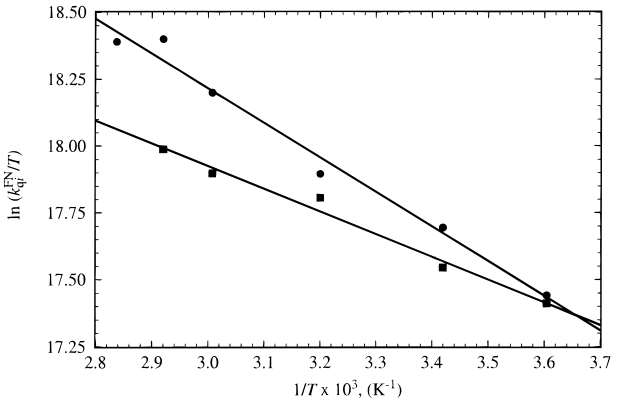

Figure 7. Transition state plots for $k_{q_i}^{FN}$ (i = A, ●, and B, ■).

Plots of the rate constants in Table 2 adhere well to eq 3 (Figure 7), yielding $\Delta H_i^{\ddagger} = 2.55 \pm 0.15$ and 1.70 ± 0.20 kcal/mol and $[(\Delta S_i^{\ddagger}/R) + \ln(\kappa_i k/h)] = 22.06 \pm 0.24$ and 20.48 ± 0.20 for t-APE$_A$ and t-APE$_B$, respectively (the 79.3 °C point was omitted for t-APE$_B$). We do not consider the difference in these two sets of parameters significant in view of experimental uncertainties in our K_{SV} values and in the experimental[3b] τ_f values. As expected for diffusion-controlled processes, both activation enthalpies are close to the activation enthalpy for viscous flow, $\Delta H_{\eta_s}^{\ddagger} = 2.11 \pm 0.01$ kcal/mol, which is based on an approximate form of Eyring's equation for η_s

$$\eta_s = (Nh/V)e^{-\Delta S\eta_s^{\ddagger}/R}e^{\Delta H\eta_s^{\ddagger}/RT} \qquad (4)$$

where V is the molar volume of the solvent.[26,27] The analogous rate constants for O_2 quenching at 20 °C in toluene adjusted for small deviations of the intercepts of the SV plots from unity that were neglected in ref 4 are $(3.39 \pm 0.13) \times 10^{10}$ and $(3.45 \pm 0.44) \times 10^{10}$ M^{-1} s^{-1} for t-APE$_A$ and t-APE$_B$, respectively. Thus, both FN and O_2 quench *t*-APE fluorescence at diffusion-controlled rates and show no selectivity between t-APE$_A$ and t-APE$_B$.[4] Differential conformer quenching is expected only when much less reactive quenchers are employed.[13,28]

Resolved Fluorescence Spectra. The shoulder at the onset of the resolved t-APE$_B$ spectra in Figure 6 becomes increasingly more prominent as the temperature of the toluene solution is raised. This spectral feature was first noted by Bartocci et al. as it is clearly evident in the unresolved *t*-APE fluorescence spectra.[3b,c] Their assignment of this shoulder to $S_2 \rightarrow S_0$ emission arising due to thermal equilibration of S_2 and S_1 states of t-APE$_B$ is no doubt correct. Entirely analogous behavior[29-31] was reported earlier for the *s-trans*,*s-trans*-conformer[32] of *all-trans*-1,6-diphenyl-1,3,5-hexatriene (*st*-DPH). In *st*-DPH, the initially excited 1^1B_u state relaxes, within at most 10 ps,[33] to an equilibrium mixture with the lower-lying 2^1A_g state and fluorescence arises from both states. Although PCA-SM treatment allows resolution of DPH fluorescence spectra into pure s-trans and s-cis conformer spectra,[32] the PCA-SM resolution of $2^1A_g \rightarrow 1^1A_g$ and $1^1B_u \rightarrow 1^1A_g$ components of the s-trans component is not straightforward.[34] The difficulty arises from the relatively strong linear dependence of the $1^1B_u \rightarrow 1^1A_g$ energy gap, ΔE_b, on the polarizability of the medium $\alpha = (n^2 - 1)/(n^2 + 2)$ where n is the index of refraction.[31,35-37] The relative contribution of the 1^1B_u emission in *st*-DPH fluorescence increases upon raising the temperature in a specific solvent or by increasing $\alpha(n)$ at constant temperature[31] by use of a series of solvents.[35-37] However, resolution of matrices of such spectra into pure $1^1B_u \rightarrow 1^1A_g$ and $2^1A_g \rightarrow 1^1A_g$ components is hampered because the 1^1B_u spectrum shifts significantly as the polarizability of the medium changes.[34]

TABLE 3: Temperature Dependence of *t*-APE Conformer Fluorescence Spectra in Toluene[a]

	t-APE$_A$		*t*-APE$_B$	
T, °C	λ_1	λ_2	λ_1	λ_2
4.3	424.0	451.0	412.0	437.2
19.3	423.0	450.0	412.0	437.0
39.3	422.8	449.6	412.0	436.0
59.3	422.0	449.0	412.0	435.0
69.3	421.0	447.8	412.0	434.6
79.3	420.8	447.0	412.0	434.0

[a] Wavelengths in nm for the λ_{max} of the two major bands in each spectrum.

A further consequence of the change in the energy gap, ΔE_{ba}, between the lowest two excited singlet states concerns the strong dependence of the mixing between these two states on ΔE_{ba}. The symmetry-forbidden nature of the $2^1A_g \rightarrow 1^1A_g$ transition that comprises the bulk of *st*-DPH fluorescence is reflected in effective radiative rate constants, $k_f^{obsd} = (\bar{\phi}_f/\tau_f)$, that depend strongly on solvent.[37−39] This behavior is accounted for by vibronic mixing of the 1^1B_u and 2^1A_g states that controls the magnitude of the $2^1A_g \rightarrow 1^1A_g$ radiative rate constant, k_{f_A}

$$k_{f_A} = k_{f_B}(V/\Delta E_{ba})^2 \qquad (5)$$

where V is the coupling matrix element and k_{f_B} is the radiative rate constant for the symmetry allowed $1^1B_u \rightarrow 1^1A_g$ transition.

The theoretical description of the two lowest excited singlet states *t*-APE$_B$ suggests a strong similarity with *st*-DPH.[3a] Here, too, the S_1 and S_2 states are nearly degenerate and the S_1 state has the lower oscillator strength.[3a] That the S_1 state borrows transition probability from the S_2 state, depending on the energy gap between the two states, is suggested by the sensitivity of τ_{f_B} on the medium: $\tau_{f_B} = 27.8 \pm 0.04$ and 64.6 ± 2.0 ns at 20 °C in toluene and methylcyclohexane/3-methylpentane (9/1, v/v) (MCH/3MP), respectively.[5] No such pronounced lifetime dependence is observed for *t*-APE$_A$ where the ordering of the two lowest excited states is reversed and S_1 state is predicted[3a] to have the strongly allowed transition.[5]

It is not surprising, therefore, that temperature-induced shifts in the UV absorption spectra of *t*-APE[2c,4] and of the naphthyl analogue, *t*-NPE,[10] thwart PCA-SM resolutions of conformer specific absorption spectra in both systems. The blue shift with increasing temperature is clearly evident in the resolved fluorescence spectra of *t*-APE$_A$ (Figure 5) as most, if not all, of its emission corresponds to a more strongly allowed transition.[3a] The temperature effect on the fluorescence spectra of *t*-APE$_B$ (Figure 6) is more complex. The first major band at 412 nm appears to be insensitive to temperature, whereas the band corresponding to the λ_{max} at ~435 nm undergoes nearly the same shift as the bands in the fluorescence spectrum of *t*-APE$_A$. The positions of the two major bands of the spectra of the two conformers are shown in Table 3. A weak shoulder at the onset of the fluorescence spectra of *t*-APE$_A$ suggests that thermal equilibrium between S_2 and S_1 states may exist in this conformer also. The $S_2 \rightarrow S_1$ transition is expected to have the lower oscillator strength in this conformer,[3a] accounting for its more subtle appearance in the fluorescence spectra.

Spalletti et al. attempted the PCA resolution of a spectrothermal matrix of *t*-APE fluorescence spectra using the maximal spectral dissimilarity SM constraint.[3d] The analysis was based on the assumption that the spectra consisted of three components: the $S_2 \rightarrow S_0$ and $S_1 \rightarrow S_0$ spectra of *t*-APE$_B$ and the $S_1 \rightarrow S_0$ spectrum of *t*-APE$_B$. It was further assumed that these three spectra are essentially invariant with temperature. A highly structured $S_2 \rightarrow S_0$ spectrum for *t*-APE$_B$ was derived.[3d]

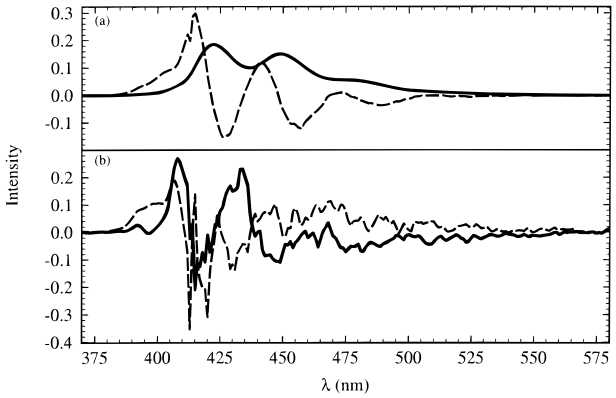

Figure 8. Four most important eigenvectors from the spectrothermal matrix of resolved *t*-APE$_A$ fluorescence spectra at different temperatures: (a) V_α (—), V_β (− − −), (b) V_γ (—), V_δ (− − −); the six largest eigenvalues are 7.258×10^{-2}, 3.493×10^{-4}, 9.887×10^{-6}, 7.506×10^{-6}, 2.187×10^{-6}, and 1.582×10^{-6}.

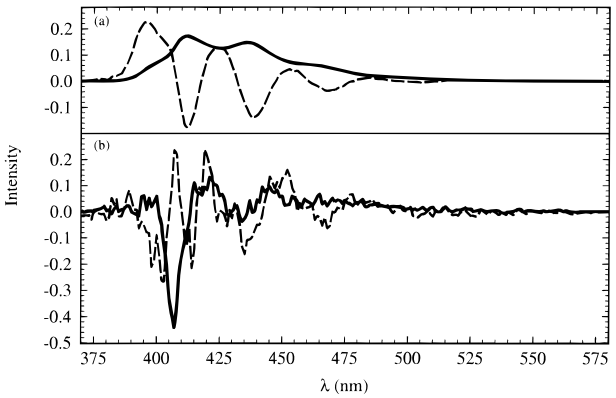

Figure 9. As in Figure 9 except for *t*-APE$_B$; the six largest eigenvalues are 7.116×10^{-2}, 2.040×10^{-4}, 6.497×10^{-6}, 1.661×10^{-6}, 9.453×10^{-7}, and 3.766×10^{-7}.

Our results allow a definitive test of the validity of this analysis. Each set of resolved spectra in Figures 5 and 6 was used separately as the input matrix for PCA. Neither set behaves as a two-component system. Figures 8 and 9 show the four most important eigenvectors for the *t*-APE$_A$ and *t*-APE$_B$ spectra, respectively. Clearly, in both cases the third and fourth eigenvectors, despite relatively small associated eigenvalues, show well-defined structure. If only the two major eigenvectors are employed, combination coefficients for the spectra in each matrix show small systematic deviations from the normalization lines. Forcing each system to a two-component solution using the LS constraint gives the apparent resolved spectra in Figures 10 and 11. That these spectra cannot be assumed to correspond to the $S_2 \rightarrow S_0$ and $S_1 \rightarrow S_0$ transitions of each conformer becomes readily apparent when one considers the inconsistency in predicted energy gaps between the S_2 and S_1 states. The relative positions of the emission bands in the derived spectra predict $\Delta E_{S_2\text{-}S_1} = 0.8$ and 2.3 kcal/mol for *t*-APE$_A$ and *t*-APE$_B$, respectively. If these values were real, they would correspond to enthalpy differences based on the fractional contributions of the derived spectra, x_{1i} and x_{2i} (where i designates conformer A or B and the numerals designate the low- and high-energy spectra) to the resolved spectra. For the fast equilibration case, the ratio of the fluorescence quantum yields is given by

$$\frac{\phi_{f2i}}{\phi_{f1i}} = \frac{k_{f2i}}{k_{f1i}} K_{21i} \qquad (6)$$

where K_{21i} is the equilibrium constant for the $S_{1i} \rightleftharpoons S_{2i}$ process

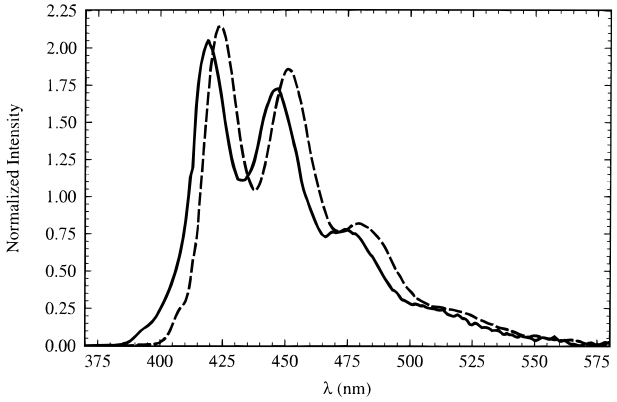

Figure 10. Apparent resolved *t*-APE$_A$ fluorescence spectra based on the erroneous premise that the spectrothermal matrix is a two-component system. Spectra are corrected for nonlinearity in instrumental response.

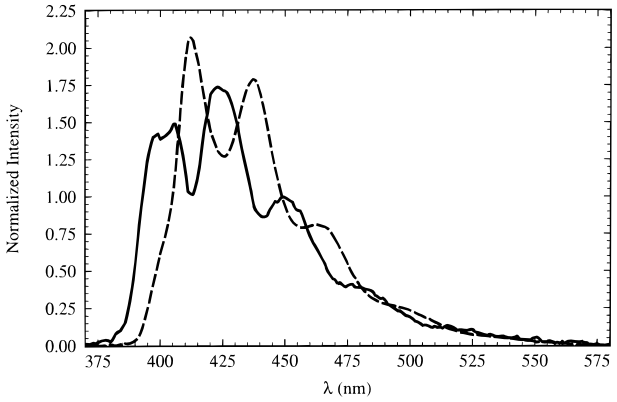

Figure 11. As in Figure 11 except for *t*-APE$_B$.

of the A or B conformer.[31] It follows that

$$\ln(x_{2i}/x_{1i}) = -(\Delta H_{21i}/RT) + \Delta S_{21i}/R + \ln(k_{f2i}/k_{f1i}) \quad (7)$$

Plots of the fractional contributions based on eq 7 (Figure 12) show systematic deviations from linearity and give anomalously large $\Delta H_{21} = 5.9$ and 8.0 kcal/mol for *t*-APE$_A$ and *t*-APE$_B$, respectively, inconsistent with the ΔE_{21} values obtained from the band positions of the derived spectra. We conclude that the PCA-SM spectral resolution of the two spectrothermal matrices fails due to temperature-induced spectral shifts and broadening in the spectra of the individual conformers. These nonlinear effects overwhelm changes in the spectra reflecting the relative population of S_2 and S_1 states. The result is analogous to that obtained on attempting to resolve spectrothermal matrices of absorption spectra of *t*-APE[2c,4] and *t*-NPE.[10]

Since it may be argued that the PCA behavior of the spectrothermal matrices of the resolved conformer spectra as multicomponent systems reflects inaccuracies in the resolutions of *t*-APE$_A$ and *t*-APE$_B$ spectra, we have also performed PCA on a global matrix consisting of all experimental spectra at all temperatures. This matrix is analogous to that employed in ref 3d with the exceptions that (a) our temperature range is smaller and (b) the presence of FN affords an additional dimension in our spectra. This global matrix too behaves as a multicomponent system, having eigenvalues for the fifth and sixth eigenvectors that are similar in magnitude to that of the fourth (caption of Figure 13). The four most significant eigenvectors are shown in Figure 13. Assuming the four-component model, the experimental spectra are represented rather well as linear combinations of these four eigenvectors. A combination coefficient plot in α, β, γ space is shown in Figure 14. Also located on this plot are the combination coefficients of the

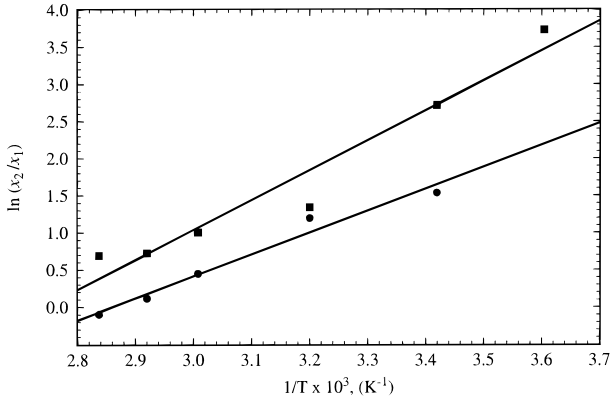

Figure 12. Plots of fractional contribution ratios based on eq 7 for *t*-APE$_A$ (●) and *t*-APE$_B$ (■).

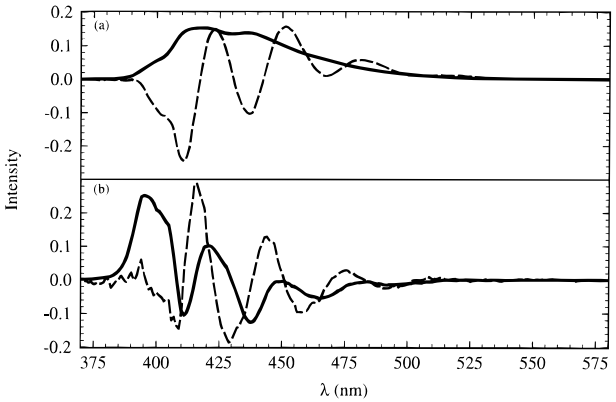

Figure 13. Four most important eigenvectors from the global spectrothermal matrix of *t*-APE fluorescence spectra. The six largest eigenvalues are 2.138, 1.008×10^{-2}, 2.977×10^{-3}, 2.873×10^{-4}, 5.453×10^{-5}, and 2.395×10^{-5}. The eigenvectors shown (see Figure 8 for legend) account for 99.99% of the total variance.

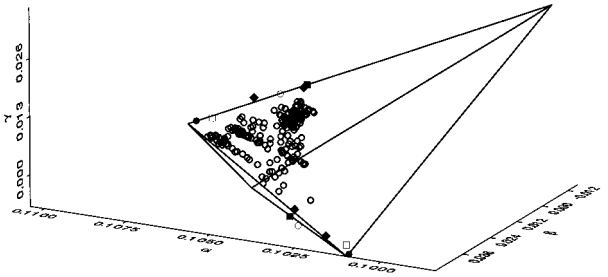

Figure 14. Combination coefficients for the global spectrothermal matrix plotted in α, β, γ space. The figure shows the tetrahedron defined by the four apparent resolved spectra in Figures 10 and 11. Experimental spectra are represented by (○); the other symbols correspond to the resolved fluorescence spectra in Figures 4−6.

resolved spectra in Figures 5 and 6 and of the derived artificial spectra in Figures 10 and 11. All of the latter combination coefficients are obtained from dot products of the normalized spectra with the eigenvectors. The points for the spectra in Figures 10 and 11 can be viewed as the corners of a tetrahedron in four-component combination coefficient space.[13] The pure component spectra in Figures 5 and 6 correspond to combination coefficients that fall sensibly close to two edges of the tetrahedron and give the appearance of a successful four-component resolution. As demonstrated above, however, this is a resolution reflecting primarily spectral shifts and broadening of the individual conformer spectra. Though the fluorescence of each conformer is dual, due to the presence of S_2 and S_1 contributions, PCA-SM is an inappropriate approach for the resolution of these emissions.

Acknowledgment. This research was supported by NSF, most recently, by Grant CHE-9612316.

References and Notes

(1) For reviews see: (a) Jacobs, H. J.; Havinga, E. *Adv. Photochem.* **1979**, *11*, 305−373. (b) Mazzucato, U.; Momicchioli, F. *Chem. Rev.* **1991**, *91*, 1679−1719.

(2) (a) Fischer, G.; Fischer, E. *J. Phys. Chem.* **198**1, *85*, 2611−2613. (b) Wismontski-Knittel, T.; Das, P. K.; Fischer, E. *J. Phys. Chem.* **1984**, *88*, 1163−1168. (c) Ghiggino, K. P.; Skilton, P. F.; Fischer, E. *J. Am. Chem. Soc.* **1986**, *108*, 1146−1149.

(3) (a) Bartocci, G.; Masetti, F.; Mazzucato, U.; Spalletti, A.; Orlandi, G.; Poggi, G. *J. Chem. Soc., Faraday Trans. 2* **1988**, *84*, 385−399. (b) Bartocci, G.; Masetti, F.; Mazzucato, U.; Baraldi, I.; Fischer, E. *J. Mol. Struct.* **1989**, *193*, 173−183. (c) Bartocci, G.; Mazzucato, U.; Spalletti, A.; Elisei, F. *Spectrochim. Acta, A* **1990**, *46*, 413−418. (d) Spalletti, A.; Bartocci, G.; Masetti, F.; Mazzucato, U.; Cruciani, G. *Chem. Phys.* **1992**, *160*, 131−144.

(4) Saltiel, J.; Zhang, Y.; Sears, D. F., Jr.; Choi, J.-O. *Res. Chem. Intermed.* **1995**, *21*, 899−921.

(5) Bartocci, G.; Mazzucato, U.; Spalletti, A. *Chem. Phys.* **1996**, *202*, 367−376.

(6) Mazzucato, U.; Spalletti, A.; Bartocci, G. *Coord. Chem. Rev.* **1993**, *125*, 251−260.

(7) Saltiel, J.; Zhang, Y.; Sears, D. F. Jr., *J. Am. Chem. Soc.* **1996**, *118*, 2811−2817.

(8) Laarhoven, W. H.; Cuppen, Th., J. H. M.; Nivard, R. J. F. *Tetrahedron* **1970**, 4865−4881.

(9) Saltiel, J.; Tarkalanov, N.; Sears, D. F., Jr. *J. Am. Chem. Soc.* **1995**, *117*, 5586−5587.

(10) Saltiel, J.; Choi, J.-O.; Sears, D. F., Jr.; Eaker, D. W.; Mallory, F. B.; Mallory, C. W. *J. Phys. Chem.* **1994**, *98*, 13162−13170.

(11) Saltiel, J.; Sears, D. F., Jr.; Choi, J.-O.; Sun, Y.-P.; Eaker, D. W. *J. Phys. Chem.* **1994**, *98*, 35−46, 8260.

(12) *International Critical Tables*; McGraw Hill: New York, 1930; Vol. III, pp 27−29, for densities and Vol. VII, p 218, for viscosities.

(13) Saltiel, J.; Choi, J.-O.; Sears, D. F., Jr., Eaker, D. W.; O'Shea, K. E.; Garcia, I. *J. Am. Chem. Soc.* **1996**, *118*, 7478−7485.

(14) (a) Green, B. S.; Rejtö, M.; Johnson, D. E.; Hoyle, C. E.; Simpson, J. T.; Correa, P. E.; Ho, T.-I.; McCoy, F.; Lewis, F. D. *J. Am. Chem. Soc.* **1979**, *101*, 3325−3331. (b) Lewis, F. D.; Simpson, J. T. *J. Phys. Chem.* **1979**, *83*, 2015−2019. (c) Hub, W.; Klüter, U.; Schneider, S.; Dörr, F.; Oxman, J. D.; Lewis, F. D. *J. Phys. Chem.* **1984**, *88*, 2308−2315.

(15) Aloisi, G. G.; Elisei, F.; Mazzucato, U.; Prats, M. *J. Photochem. Photobiol. A. Chem.* **1991**, *62*, 217−228.

(16) (a) Adams, B. K.; Cherry, W. R. *J. Am. Chem. Soc.* **1981**, *103*, 6904−6907. (b) Arnold, D. R.; Wong, P. C. *J. Am. Chem. Soc.* **1979**, *101*, 1894−1895.

(17) Goodman, J. L.; Peters, K. S. *J. Am. Chem. Soc.* **1985**, *107*, 1441−1442.

(18) (a) Birks, J. B.; Bartocci, G.; Aloisi, G. G.; Dellonte, S.; Barigelletti, F. *Chem. Phys.* **1980**, *51*, 113−120. (b) Bartocci, G.; Masetti, F.; Mazzucato, U.; Spalletti, A.; Bruni, M. C. *J. Chem. Soc., Faraday Trans 2*, **1986**, *82*, 775−788. (c) Bartocci, G.; Mazzucato, U.; Masetti, F.; Aloisi, G. G. *Chem. Phys.* **1986**, *101*, 461−466.

(19) Saltiel, J.; Waller, A. S.; Sears, D. F., Jr.; Garrett, C. Z. *J. Phys. Chem.* **1993**, *97*, 2516-2522 and references cited therein.

(20) Saltiel, J.; Atwater, B. W. *Adv. Photochem.* **1988**, *14*, 1−90.

(21) Lehni, M.; Schuh, H.; Fischer, H. *J. Chem. Kinet.* **1979**, *11*, 705−713.

(22) Weller, A. *Z. Phys. Chem. NF* **1957**, *13*, 335−352.

(23) Hui, M.-H.; Ware, W. R. *J. Am. Chem. Soc.* **1976**, *98*, 4718−4727.

(24) Andre, J. C.; Niclause, M.; Ware, W. R. *Chem. Phys.* **1978**, *28*, 371−377.

(25) Bohne, C.; Kennedy, S. R.; Boch, R.; Negri, F.; Orlandi; G.; Siebrand, W.; Scaiano, J. C. *J. Phys. Chem.* **1991**, *95*, 10300−10306.

(26) (a) Eyring, H. *J. Chem. Phys.* **1936**, *4*, 283−291. (b) Kauzmann, W.; Eyring, H. *J. Am. Chem. Soc.* **1940**, *62*, 3113−3125.

(27) Kierstead, H. A.; Turkevich, J. *J. Chem. Phys.* **1944**, *12*, 24−27.

(28) Sun, Y.-P; Sears, D. F., Jr.; Saltiel, J.; Mallory, F. B.; Mallory, C. W.; Buser, C. A. *J. Am. Chem. Soc.* **1988**, *110*, 6974−6984.

(29) (a) Alford, P. C.; Palmer, T. F. *Chem. Phys. Lett.* **1982**, *86*, 248−253. (b) Alford, P. C.; Palmer, T. F. *J. Chem. Soc., Faraday Trans. 2* **1983**, *79*, 433−447.

(30) Jones, G. R.; Cundall, R. B. *Chem. Phys. Lett.* **1986**, *126*, 129−133.

(31) Itoh, T.; Kohler, B. E. *J. Phys. Chem.* **1987**, *91*, 1760−1764.

(32) Saltiel, J.; Sears, D. F., Jr.; Sun, Y. P.; Choi, J.-O. *J. Am. Chem. Soc.* **1992**, *114*, 3607-3612.

(33) Hilinski, E. F.; McGowan, W. M.; Sears, D. F., Jr.; Saltiel, J. *J. Phys. Chem.* **1996**, *100*, 3308−3311.

(34) Saltiel, J.; Sears, D. F.; Sun, Y.-P.; Choi, J.-O.; Garcia, I. Unpublished results.

(35) Sklar, L. A.; Hudson, B.; Petersen, M.; Diamond, J. *Biochemistry* **1977**, *16*, 813−828.

(36) Andrews, J. R.; Hudson, B. S. *J. Chem. Phys.* **1978**, *68*, 4587−4594.

(37) Hudson, B. S.; Kohler, B. E.; Schulten, K. In *Excited States*; Lim, E. C., Ed.; Academic Press: New York, 1982; Vol. 6, pp 1−95.

(38) Hudson, B. S.; Kohler, B. E. *J. Chem. Phys.* **1973**, *59*, 4984−5002.

(39) Birks, J. B.; Tripathi, G. N. R.; Lumb, M. D. *Chem. Phys.* **1978**, *33*, 185−194.

(40) Sun, Y.-P.; Sears, D. F., Jr.; Saltiel, J. *J. Am. Chem. Soc.* **1989**, *111*, 706−711.